# BLOCK ADJUSTEMENT OF LANDSAT-7 ETM+ IMAGES

Thierry Toutin, Yves Carbonneau* and René Chénier*
Natural Resources Canada, Canada Centre for Remote Sensing
588 Booth Street, Ottawa, Ontario, Canada, K1A 0Y7
thierry.toutin@ccts.nrcan.gc.ca

**KEY WORDS**

Bundle block adjustment, Geometric evaluation, Error propagation, Landsat-7

**ABSTRACT**

This research study shows the potential of large image-block adjustment with nadir viewing sensor images. The method uses the geometric correction system developed for multi-source images at the Canada Centre for Remote Sensing.  The results with 15 Landsat-7 ETM+ images show that the same accuracy can be obtained with a large image block than with a single image using the same number of ground control points (GCPs).  The number of GCPs depends on cartographic data accuracy to reduce the propagation of GCP error in the least-square block adjustment. To insure consistency and convergence in the block adjustment, strips of same-path and date images has to be generated. Furthermore, elevation tie points (with known elevation value) are used in the overlaps (North-South and East-West) because the viewing-angle differences of overlapping images are small: less than 1º in North-South overlaps and less than 10º in East-West overlaps.

# 1. INTRODUCTION

Such as in photogrammetry where strips and block of aerial photos are processed together, it seems normal to perform the same process with satellite images from same and/or adjacent orbits. The geometric processing is realized with an image block adjustment instead of a single image adjustment.  This spatio-triangulation process was first developed and tested with off-nadir viewing SPOT images (Toutin, 1985; Veillet, 1991) and with along-track stereo MOMS images (Kornus *et al.*, 2000), and generally in a research context or by governmental agencies. Few results were presented neither with nadir viewing images or in an operational environment.  Due to new and low-cost Landsat-7 data, it seems interesting to adapt the method for this data and to develop operational strategies in an user-friendly and robust system.

There are different advantages to block adjustment:
➢ To reduce the number of ground control points (GCPs);
➢ To obtain a better relative accuracy between the images;
➢ To obtain a more homogeneous and precise mosaic over large areas; and
➢ To generate homogeneous GCP network for future geometric processing.

The spatio-triangulation process is based on a bundle adjustment of all images combined with ground control and orbit information. With the spatio-triangulation, the same number of GCPs is theoretically needed to correct a single image, an image strip or a block: 6 GCPs are enough for Landsat-7 (Cheng *et al.*, 2000). However, in operational context, it is better to use twice more when they are precise due to potential error in their identification and plotting, and more when they are less precise.  The least-square block adjustment will thus reduce their error propagation.

---

* Under contract with Consultants TGIS inc., 7667 Curé Clermont, Anjou (Québec) H1K 1X2, Canada

This paper will present the method to generate and process image strips and block from Landsat-7 ETM[+] images. Comparative results between the processing of a single image, image strip(s) or block are presented to validate the stability and robustness of the system. The mathematical tool used is the geometric correction developed at the Canada Centre for Remote Sensing (CCRS) for multi-source images (Toutin, 1995) and adapted to Landsat-7 ETM[+] images (Cheng *et al.*, 2000). Different strategies are also presented for operational uses.


## 2. GENERATION OF STRIPS AND BLOCK

**Image-strip generation**

Since satellite data are acquired in a continuous strip the data should be delivered in such long strip. However, they are "artificially" cut into square images, the images from a same orbit and from a same acquisition date has to be stitched to re-create the continuous strip in the North-South direction (Sakaino *et al.*, 2000). However, the 1G images are geo-referenced, e.g., projected along the ground orbit track at the image centre, there is a different azimuth for each image, and the lines in the overlap area do not superimpose any more. A matching technique (visual or automatic) has then to be used in the overlap area to compute the rotation-translation in order to stitch the images.

Theoretically, there is no limit to the number of images to be stitched when they are acquired the same date, but practically due to the 1G pre-processing and the cloud coverage, no more than 5 images can be stitched together in about 900-km strip. When the images are acquired from different dates then from different physical orbits, they cannot be stitched in a same strip. Another method with tie points (TP) must be applied to create a link between the images in the North-South direction. However, the stereo-geometry will be weak with base-to-height (B/H) ratio less than $10^{-3}$.

**Image-block generation**

Finally, blocks are generated from images or strips in the East-West direction acquired from adjacent paths. The link between images/strips is realised with TP Since Landsat ETM[+] images are acquired at nadir the intersection angles are 10°-15° depending of the latitude, generating B/H ratios of 0.13-0.25. Consequently, it is necessary to use TP with a known elevation in both directions (North-South, East-West) in order to strength the intersection geometry between the two images and the ground. In operational conditions, use of elevation TP becomes mandatory to avoid error propagation and to obtain a better stability in this weak stereo-geometry. However, some TPs can also be added in East-West directions only. For this block, there are 12 and 10 overlaps in the East/West and North/South directions respectively, when the block is formed with separate images, are 11 and 5 overlaps in the East/West and North/South directions, respectively when the block is formed with strips.


## 3. DATA SET

15 ETM[+] panchromatic images with 15-m pixel spacing were acquired over the Rocky Mountains, Canada from Vancouver in the south-west to Calgary at the north-east. They are level 1G systematically georeferenced and oriented along the orbit track. They generate a block with five paths and three rows (Figure 1). Some paths have two or three images of the same date (outlined in Figure 1) and one path has images from three dates. It enables different images/strips/block configurations to be tested. The North/South and East/West overlaps are around 10% and 40%, respectively. The images cover an area of 600 km by 500 km, and the elevation variation is 2 500 m. Cartographic data are 350 topographic maps at 1:50 000 with 25-50 m accuracy. About 55 ground points per image were collected. A DEM (50-m grid spacing) was generated from the contour lines of 1:250 000 maps with an error of 50 m. This 50-m error will generate less than 10-m positioning error in the geocoding process of each image (view angle less than 7.5º at the image border).
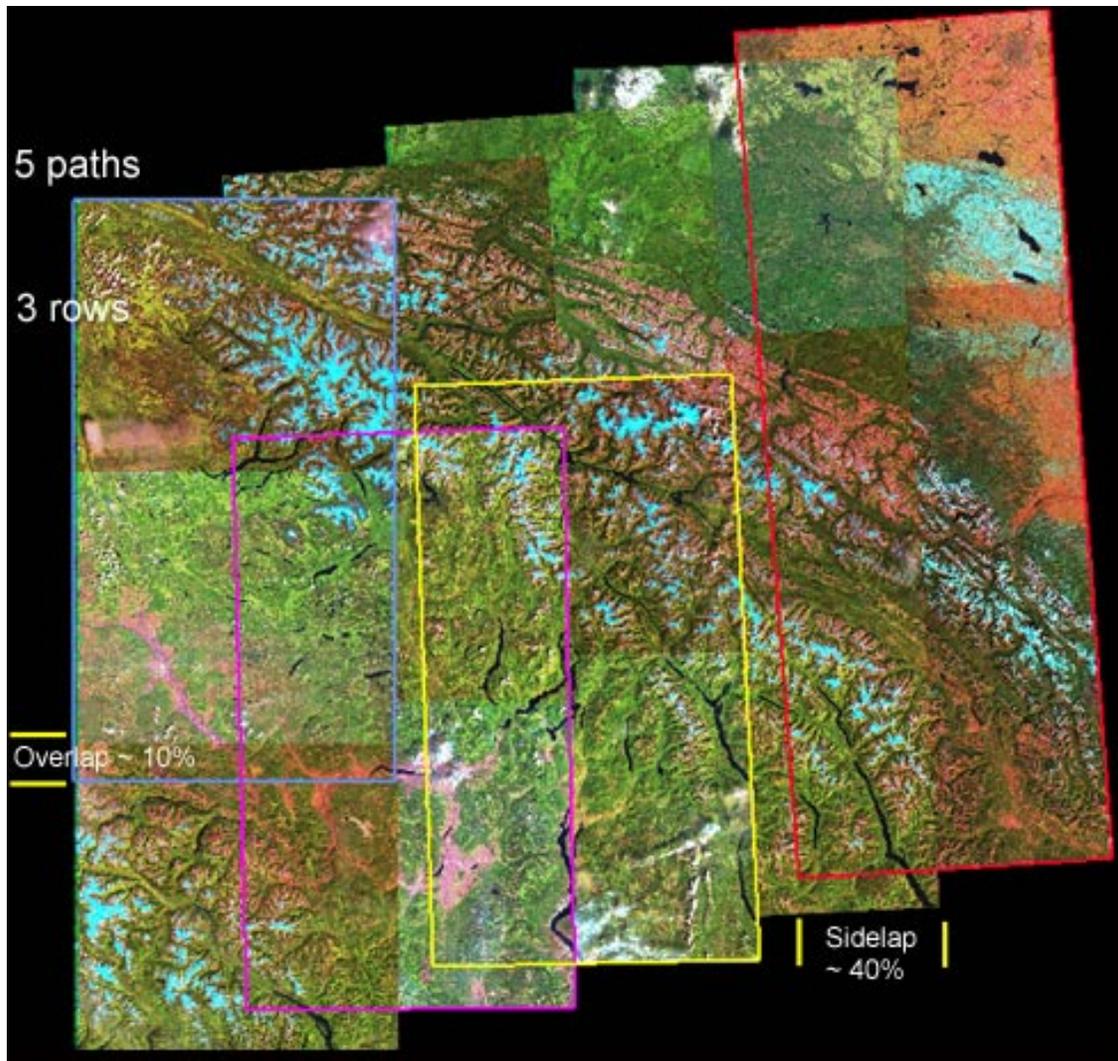
Figure 1: Study site and Landsat-7 ETM[+] images over the Canadian Rocky Mountains, Canada. The coloured outlines determinates the 2- or 3 image strips from same path and date.

## 4. RESULTS AND INTERPRETATION

The first results are given with the least-square bundle adjustment with all GCPs for different numbers and configuration of image(s) and strip(s): a single image, two or three images, two or three image strip and the whole image bloc. Table 1 gives the root mean square (RMS) and minimum/maximum residuals on these different configurations. The results for each configuration (image(s) or strips) correspond to the mean of results for all possibilities for this configuration (e.g., the result for a single image is the mean of results of 15 single images). In the block adjustment, GCPs belonging to more than one image is also used as TP.

These coherent results demonstrate the applicability of the geometric model and of the system to Landsat-7 block adjustment, but also a good stability and robustness of the method, whatever the image/strip/block configuration because all residuals are equivalent. Since they are in the same order than the cartographic data error (25 m), the GCP error did not propagate through the geometric model but in the residuals, due to the redundancy in the least-square adjustment.

Tableau 1: Root mean square (RMS) and minimum/maximum residuals on GCPs (in metres) of the least-square adjustments for different image/strip configurations

| Least-square adjustment | GCPs | RMS Residuals | | Min/Max Residuals | |
|---|---|---|---|---|---|
| | | X | Y | X | Y |
| 1 image single | 55 | 20.8 | 18.9 | -59/49 | -45/47 |
| 2 images N/S | 110 | 21.5 | 19.8 | -41/52 | -41/43 |
| 3 images N/S | 165 | 20.0 | 19.2 | -43/48 | -49/44 |
| 3 images E/W | 165 | 19.8 | 19.5 | -45/46 | -50/48 |
| 2-image strip | 110 | 23.2 | 22.5 | -35/45 | -49/37 |
| 3-image strip | 165 | 23.0 | 20.6 | -41/48 | -41/44 |
| 15-image block | 800 | 22.6 | 21.2 | -59/52 | -49/47 |

To find the appropriate number of GCPs as a function of their cartographic errors, different tests are performed by varying the GCP number. A 3-image strip was used because it has the largest number of GCPs (148). Points not used as GCP are used as independent check points (ICPs) to verify the model error. Figure 2 gives the RMS X-Y residuals (in metres) on GCPs varying from 148 to 10 in the least-square strip adjustment, and RMS X-Y errors (in metres) on ICPs varying from 0 to 138, respectively. From 148 to 30-35 GCPs the RMS errors are equivalent with only 2-3 m variations, while 10 GCPs give RMS errors 20% worse. 25-30 GCPs are then a good compromise to avoid the propagation of GCP errors and to keep about 25-m error for the bundle adjustment.
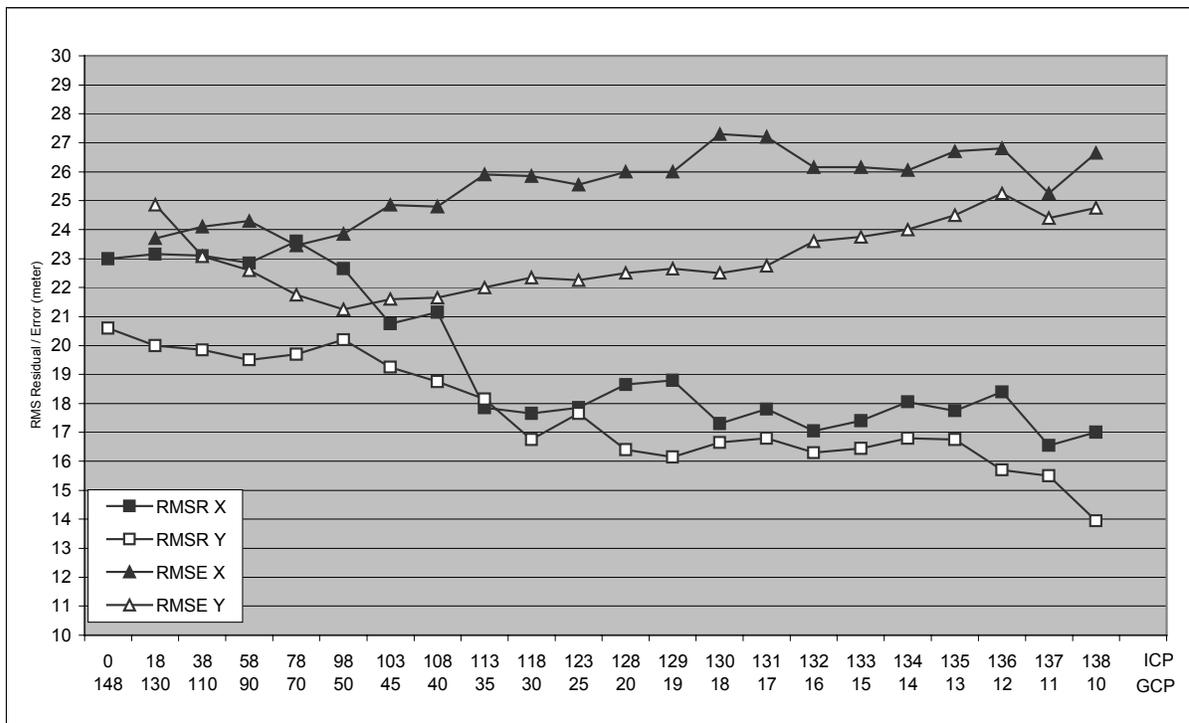


Figure 2: RMS X-Y residuals (in metres) on GCPs varying from 148 to 10 in the least-square strip adjustment, and RMS X-Y errors (in metres) on ICPs varying from 0 to 138, respectively

This result of 25 GCPs is then applied to tests different block adjustment combined with images and/or strips:
1. Three separate images in the North/South or East/West directions with 25 GCPs on the 2 outer images and 10-20 elevation TPs in the overlap areas (Figures 3 and 4, respectively);
2. Block with 15 images linked with 10-15 elevation TPs (Figures 5 and 6); and
3. Block with images and 2/3-image strips linked with 10-15 elevation TPs (Figures 7 and 8, respectively).
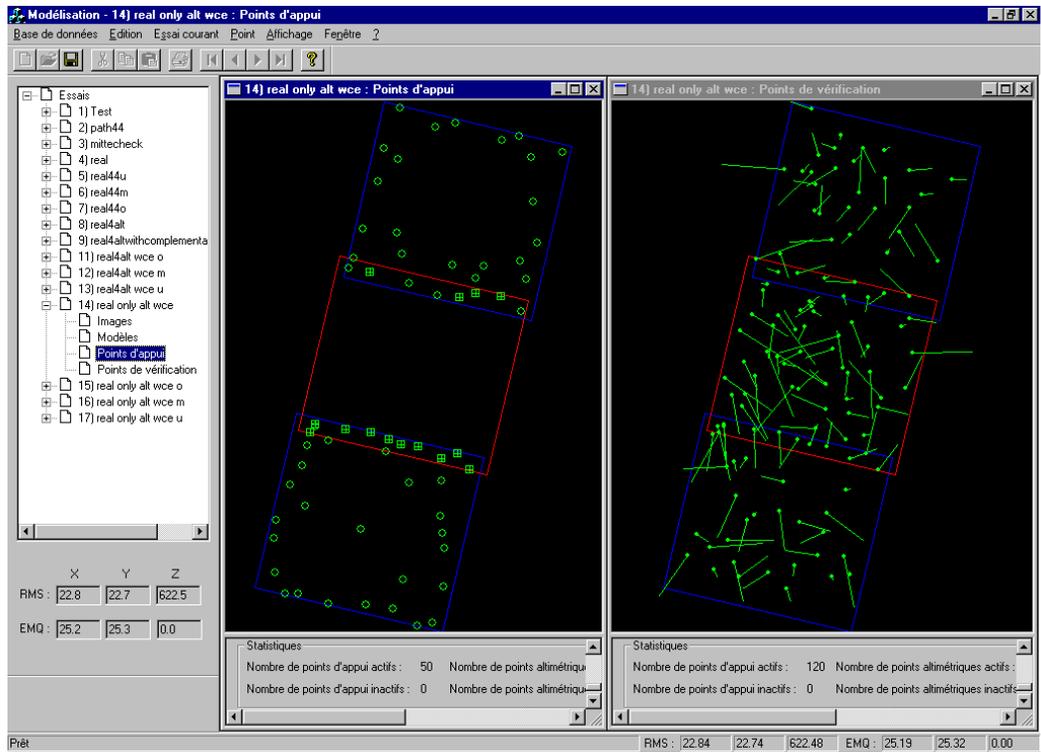
Figure 3: GCPs distribution (left window) and ICP error vectors (right window) of the block adjustment of 3 images in North/South direction with 25 GCPs on the outer images and 10 elevation TP in each overlap
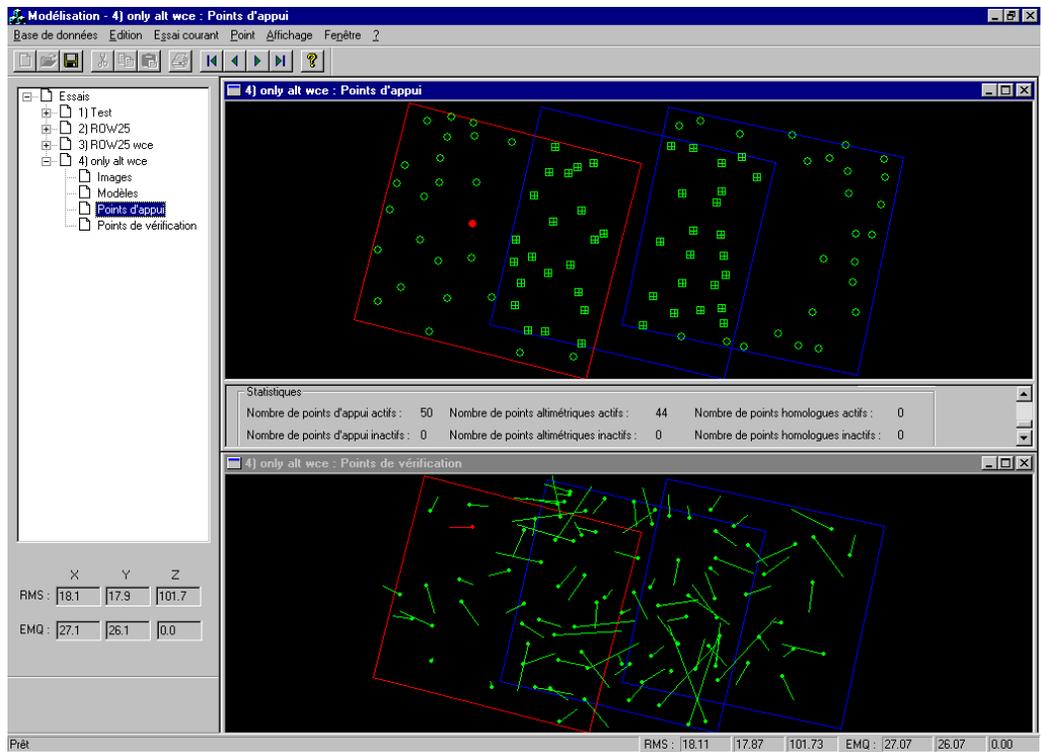


Figure 4: CPs distribution (top window) and ICP error vectors (bottom window) of the block adjustment of three images in East/West direction with 25 GCPs on the outer images and 20 elevation TP in each overlap
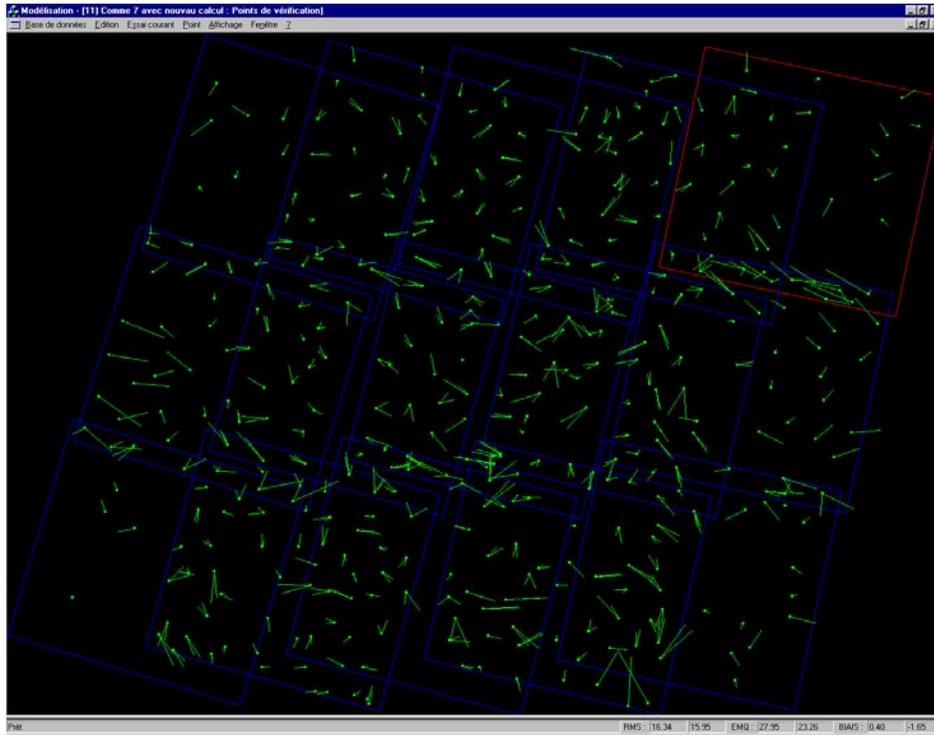
Figure 5: ICP error vectors of the 15-image block adjustment (a) with 25 GCPs every two images and with 10 elevation TP and 5-10 TPs in each overlap
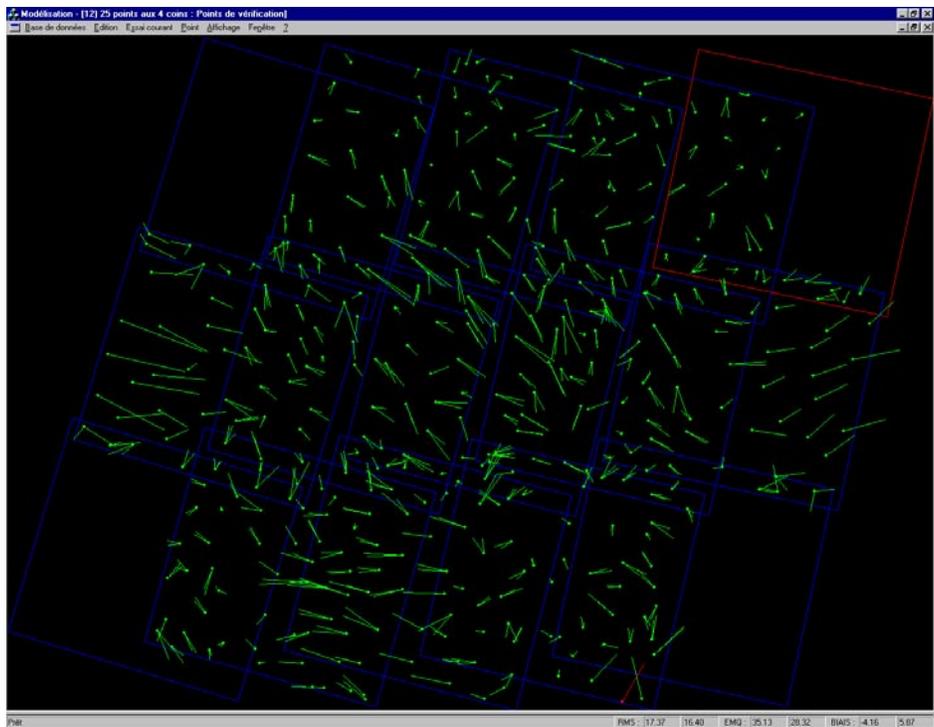


Figure 6: ICP error vectors of the 15-image block adjustment (b) with 25 GCPs in the 4 outer images and with 15 elevation TP in each overlap
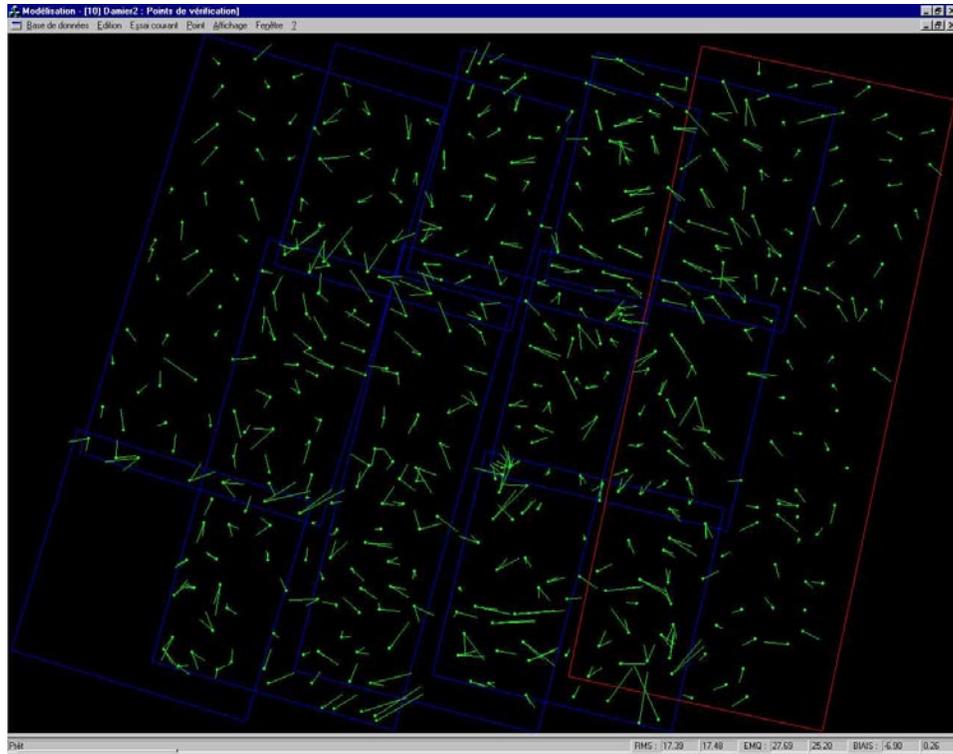
Figure 7: ICP error vectors of the image/strip block adjustment (a) with 25 GCPs every two images/strips, and with 10 elevation TP and 5-10 TPs in each overlap
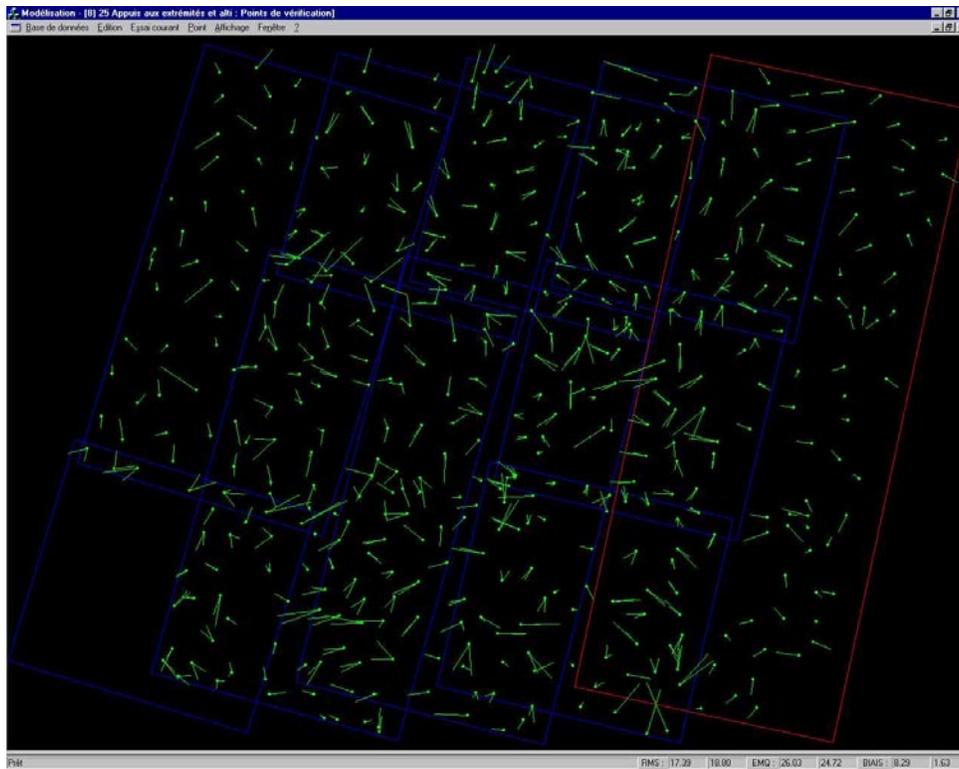


Figure 8: ICP error vectors of the image/strip block adjustment (b) with 25 GCPs in the 3 outer image/strips and 15 elevation TP in each overlap

Figures 3 and 4 show two main windows: one with the GCPs (circle), elevation TPs (square) and TPs (triangle) distribution and the second with the ICP vector errors. For clarity due to the large number of points, Figures 5 to 8 only show the ICP vector errors. In addition for the block adjustment, two tests were performed using 25 GCPs (a) every two images (Figures 5 and 7) or (b) in the outer images/strips (Figures 6 and 8). For every test, the images without GCP are linked with about 10-20 elevation TPs on each overlap. However, since the block test (b) is the most extreme configuration, a little more elevation TPs are used. Conversely, few TPs (5-10) are added in the block test (a) to obtain the same number of "links" between images, but only in the East/West overlaps because the North/South overlaps display a weak stereo-geometry ($B/H \approx 10^{-3}$ or $10^{-5}$). The RMS GCP residuals and RMS ICP errors are synthesised in Table 2 for the five bundle adjustments.

Table 2: RMS residuals (in metres) on GCPs and RMS errors (in metres) on about ICPs of the least-square adjustments for different image/strip configurations. Tests (a) and (b) correspond to two different GCP distributions in the block: (a) with GCPs every two images/strips and (b) with GCPs on the outer images/strips.

| Least-square adjustment | Figure Number | Number of GCP/ETP/TP | RMS Residuals X | Y | Number of ICPs | RMS Errors X | Y |
|---|---|---|---|---|---|---|---|
| 3 images North/South | 3 | 50/20/0 | 22.8 | 22.7 | 120 | 25.2 | 25.3 |
| 3 images East/West | 4 | 50/44/10 | 18.1 | 17.9 | 100 | 27.1 | 26.1 |
| 15-image block (a) | 5 | 200/160/80 | 16.3 | 16.0 | 600 | 28.0 | 23.3 |
| 15-image block (b) | 6 | 100/200/0 | 17.4 | 16.4 | 700 | 35.1 | 28.3 |
| Image/strip block (a) | 7 | 150/160/80 | 17.4 | 17.5 | 650 | 27.6 | 25.1 |
| Image/strip block (b) | 8 | 75/265/0 | 17.4 | 18.8 | 725 | 26.0 | 24.7 |

Table-2 results show a general coherency and confirm Table-1 results and interpretation: applicability of the model, stability and robustness of the method whatever the image/strip configurations, but also now whatever the GCP/TP distributions. A general error of 25-30 m is obtained, but which included the cartographic error of GCPs/ICPs. The two 15-image block adjustments with "weaker links" between the North/South images of same path and date ($B/H \approx 10^{-5}$) give the "worse" results (30-35 m), and especially the block (b) where only GCPs on the outer images/strips are used (no GCP in-between 360-400 km). The different Figures (3 to 8) demonstrate there is no bias/systematic error in any strip/block adjustment, and that the vector errors are similar for all images/strips with or without GCPs. Statistical evaluations for each image independently confirm this last statement. Furthermore, ICP error-vector for points belonging to two images or more are in the same direction, demonstrating a good superposition between the images. Since better results are not obtained for the images with GCPs, the block adjustment method performs well in term of relative and absolute accuracy.

## 5. CONCLUSIONS

A method of spatio-triangulation using a block bundle adjustment has been tested with 15 Landsat-7 ETM[+] panchromatic level-1G images over the Canadian Rocky Mountains. Firstly, the method to create strips and block from images of same path but from same or different dates was given. The bundle adjustment was then tested with single or multiple images and strips. Same results were obtained with a single image or 15-image block, and they were on the same order than the cartographic data accuracy (25-30 m). Other test shows that 25-30 GCPs are a good compromise to not propagate the GCP error in the image/strip adjustment. Different block/bundle adjustments were then performed with 25 GCPs, but with different distributions in the block. The whole results demonstrate the applicability of the bundle adjustment model as well as the stability and robustness of the method with nadir viewing images, whatever the number of images, the overlap directions (North/South or East/West), the image/strip configurations, and the GCP/TP distributions. A general error of 25-30 m is obtained, but which included the cartographic error of ICPs. In operational environment, it is a requisite to generate strips from images of the same path and date, and to exclusively use elevation TPs in overlapping areas

in both directions (North/South and East/West) for a greater stability and robustness. Furthermore, less GCPs are required with strips block than with images block.

## References

Kornus W., Lehner M., and Schroeder M., 2000. Geometric in-flight calibration of the stereoscopic line-CCD scanner MOMS-2P. ISPRS Journal of Photogrammetry and Remote Sensing, Vol. 55, No. 1, pp. 59-71

Sakaino S., Suzuki H., Cheng P., and Toutin Th., 2000. "Updating maps of Kazakhstan using stitched SPOT images", Earth Observation Magazine, Vol. 9, No. 3, pp. 11-13.

Toutin, Th., 1985. Analyse mathématique des capacités stéréoscopiques du système SPOT. Thèse de Docteur-ingénieur, Ecole Nationale des Sciences Géodésiques, Paris, France, 163 pages.

Toutin, Th., 1995. Multisource data fusion with an integrated and unified geometric model. EARSeL Journal Advances in Remote Sensing, Vol. 4, pp. 118-129. ww.ccrs.nrcan.gc.ca/ccrs/eduref/ref/bibpdf/1223.pdf.

Cheng Ph., Toutin, Th., and Tom V., 2000. Unlocking the Potential of Landsat 7 Data. Earth Observation Magazine, Vol. 9, No. 2, pp. 28-31. www.ccrs.nrcan.gc.ca/ccrs/eduref/ref/bibpdf/4769.pdf.

Veillet, I., 1991. Triangulation spatiale de blocs d'images SPOT. Thèse de Doctorat, Observatoire de Paris, Paris, France, 101 pages.